CHAPTER IV

ELECTRORHEOLOGICAL PROPERTIES OF POLYANILINE SUSPENSIONS: FIELD-INDUCED LIQUID TO SOLID TRANSITION AND RESIDUAL STRUCTURE

4.1 Abstract

Polyaniline (PANI) was synthesized via oxidative coupling polymerization in acid conditions and de-doped in solution of ammonia. The electrorheological (ER) properties of the PANI/silicone oil suspensions were investigated in oscillatory shear as functions of electric field strength, particle concentration, and host fluid viscosity. Consistent with literature, the PANI ER fluid exhibits viscoelastic behavior under the applied electric field and the ER response is strongly enhanced with increasing electric field strength and particle concentration. The dynamic moduli, G' and G" increase dramatically, by 5 orders of magnitude, as the electric field strength is increased to 2 kV/mm. A viscoelastic liquid to solid transition occurs at a critical electric field strength, in the range E_c = 50-200 V/mm, whose value depends on particle concentration and host fluid viscosity. The fibrillar structure formed in the presence of the applied field has a static yield strength τ_y, whose value scales with electric field strength as $\tau_y \sim E^{1.88}$. When the field is switched off a residual structure remains, whose yield stress increases with the strength of the applied field and particle concentration. When the applied stress exceeds the yield stress of the residual structure, fast, fully reversible switching of the ER response is obtained.

KEYWORDS: Electrorheological fluid, Conductive polymer, Polyaniline, Sol to gel transition

4.2 Introduction

Electrorheological (ER) suspensions, first studied extensively by Winslow (1949), display dramatic changes in rheological properties under a sufficiently large electric field (Klingenberg, 1993). A typical ER fluid is a suspension of micron-sized polarizable particles dispersed in a non-conducting medium. The mismatches in conductivity and dielectric permittivity between the dispersed particles and the continuous medium induce dipolar polarization in the particles upon application of an electric field. Under the action of the field, the induced dipoles tend to attract neighboring particles and this causes the particles to form fibrillar three dimensional network structures, which are aligned along the direction of the electric field and generate additional resistance against fluid motion (Tao and Sun, 1991, *Lee et al.*, 1998). The time scale for this transition is of the order of milliseconds (Klingenberg *et al.*, 1993). Because of the controllable viscosity and the fast response, ER fluids are regarded as smart materials with potential for application in active devices which transform electric energy to mechanical energy (Choi *et al.*, 1998). Possible applications include clutches, breaks, shock absorbers, engine mounts, valves, flow pumps, and other variable control and servo devices (Jang *et al.*, 1998).

Experimental data for the dynamic response of ER fluids are limited relative to that for steady shear flow. Small amplitude oscillatory shear experiments are more effective methods to investigate viscoelastic phenomena associated with the intact fibrillar structure; the application of small strains allows one to probe the particle interactions while minimizing the influence of the external flow field (Chin and Winter, 2002).

In suspensions of many inorganic particles, an activator, such as water or other polar compound adsorbed on the particle surface, is required to improve the ER properties. On the other hand, a semiconducting polymer usually has a high intrinsic polarizability, even in the absence of any activator [8]. Examples include polyaniline (PANI) and many PANI derivatives, based upon modification of oxidation state, dopant, and polymerization conditions (Lee *et al.*, 1998, Choi *et al.*, 1998, Jang *et al.*, 2001, Gow and Zukoski, 1990, Gozdalik *et al.*, 2000, Akhavan and Slack, 2001, Kim *et al.*, 2000, Lee *et al.*, 2001, Lengalova *et al.*, 2003, Cho *et al.*, 2004), polythiophene

(Chotpattananont et al., 2003,2004), and polyparaphenylene (Sim *et al.*, 2001, Chin *et al.*, 1998). PANI has several advantages over other polymer particles such as low density, ease of conductivity control, and thermal and environmental stability. PANI can be easily polymerized by an oxidative polymerization at relatively low temperatures and can be doped from an insulating state to a conducting state by using simple protonic acids. This allows a controlled variation in the particle dielectric constant and conductivity while keeping all other particle properties and suspension characteristics constant (Jang *et al.*, 2001).

In a previous study of the ER properties of polythiophene suspensions (Chotpattananont *et al.*, 2003), it was observed in small-amplitude controlled-strain oscillatory measurements, that, when the electric field is switched off, a substantial shear modulus is observed, indicating the existence of residual structure. Such an effect was not observed in corresponding controlled stress experiments (Chotpattananont *et al.*, 2004), presumably because the applied stress exceeded the yield stress of the residual structure.

In this study, we describe the synthesis and characterization of PANI, and investigate the ER properties under oscillatory shear deformation in the linear viscoelastic regime. We focus particularly on the effects of particle concentration, and silicone oil viscosity on the storage and loss moduli, and identification of the sol-gel transition driven by the electric field. We further investigate the switching characteristics of the ER response and confirm the existence of residual gel structure when the field is switched off, if the applied stress is too small. The dependence of the yield stress of this residual structure on particle concentration and field strength is studied.

4.3 Experimental

4.3.1 Materials

Aniline, C_6H_7N (AR grade, Merck) was vacuum-distilled and used as the monomer. Ammonium peroxydisulphate, $(NH_4)_2S_2O_8$ (AR grade, Merck) was used as the oxidant. 38 % Hydrochloric acid, HCl (AR grade, Labscan); 25 % solution of ammonia, NH_4OH (Ar grade, Merck) and methanol, CH_3OH (AR grade,

Labscan) were used as received. The base fluids, silicone oil (AR grade, Dow corning) with density 0.96 g/cm^3 and kinematic viscosities of 100, 500 and 1000 cSt were vacuum-dried and stored in a desiccator prior to use.

4.3.2 Polymerization Procedure

PANI was synthesized via an oxidative coupling polymerization according to the method of Cao *et al.*(1989) . 20.4 g of distilled aniline was added to 250 ml of 1.5M HCl and the mixture was vigorously stirred and cooled to 0-5 °C in a 3-necked round bottom flask. 250 ml of 1.5M HCl solution containing 25.5 g $(NH_4)_2S_2O_8$ was then added dropwise to the flask within an hour. After the total amount of the oxidant had been added, the reaction mixture was stirred at 0-5 °C for 4 hours. The precipitated PANI was recovered from the polymerization flask, filtered and then washed with distilled water until the washing liquid was completely colorless. To remove oligomers and other organic byproducts, the precipitate was washed with methanol several times until the methanol solution was colorless. The precipitate was then dedoped by immersion in 3% NH_4OH, washed until the washing liquid was neutral, and subsequently dried at room temperature for 48 hours in a vacuum oven, until its electrical conductivity no longer depends on drying time, before being passed through a 38 μm sieve shaker to control the particle size and its distribution.

4.3.3 Preparation of ER fluids

Prior to mixing in silicone oil, PANI powder was dried for 2 days at room temperature to remove moisture in a vacuum oven at room temperature. The particles were then dispersed in the silicone oil with an ultrasonicator for 30 minutes at 25 °C. The PANI suspensions were then prepared at volume fractions of 0.024 and 0.048. The suspensions were stored in a dessiccator and redispersed by ultrasonification for a period of 10 minutes at 25 °C before each experiment.

4.3.4 Characterization Methods

Fourier transform infrared spectroscopy (FT-IR, Bruker, Equinox 55/FRA 1065) was used to confirm the chemical structure of PANI. The spectrometer was operated in the transmission mode averaging 32 scans at a resolution of ± 4 cm^{-1}, covering a wavenumber range of 400-4000 cm^{-1} using a deuterated triglycine sulfate detector. Optical grade KBr (Carlo Erba Reagent) was

used as a background material. The samples were ground with KBr and pressed to form pellets.

Ultra Violet-Visible-near Infrared Spectra were recorded with a UV spectrometer (UV-Vis, Shimadzu, UV2550) using deuterium as the light source and a slit width of 2.0 nm. The spectra were recorded in the wavelength range between 300-900 nm at a scan speed of 240 nm/min.

Thermogravimetric analysis (TGA) data was performed using a thermogravimetric differential thermal analyzer (RIS Diamond TG-DTA, High Temp 11), at a heating rate of 10 °C/min, under nitrogen, from 30 °C to 750 °C.

The particle size distribution of PANI powder was determined by a particle size analyzer (Malvern, Master Sizer X).

Scanning electron microscopy (SEM, JEOL, JSM-5200-2AE) was used at an acceleration voltage of 10 kV and a magnification of 350 to investigate the morphology of PANI particles. Prior to observation, samples were gold sputtered.

To determine the electrical conductivity, PANI powder was pressed into disk pellets by a hydraulic press (diameter of 25 mm and ~0.2 mm thick). Electrical conductivity was measured using a custom-built four-point probe at 30 °C. The measurements were performed in the linear Ohmic regime where the specific conductivity values are independent of the applied DC voltage.

Dynamic rheological properties of the suspensions were investigated using a controlled-strain fluids rheometer (ARES, Rheometric Scientific Inc.) with a custom-built copper parallel plate geometry (diameter of 50 mm) attached to insulating spacers which are connected to the transducer or motor. The electric field for ER measurement was applied using a high voltage power supply (Source Meter, Keithley 2410). In order to study the temporal switching response of the suspension and the yield stress of the residual gel structure, a fluid stress controlled rheometer (Carrimed, CR50) with 4 cm diameter parallel plate geometry was used. In each rheometer, the voltage amplitude could be precisely controlled in the range of 0-1 kV corresponding to an electric field E = 0-2 kV/mm. The electric field was applied for 10 minutes to obtain an equilibrium fibrillar or columnar structure before each measurement was taken. The samples were first tested for viscoelastic linearity by strain sweep mode tests. The resulting stress was decomposed into in-phase and out-

of-phase contributions, the storage and loss moduli, G' and G". The experiments were carried out in the frequency sweep mode with frequency (ω) ranging from 0.1 to 100 rad/s at a temperature of 25 ± 1 °C to investigate the effect of electric field strength on G' and G". The temporal response of the suspension was also studied in the time sweep mode during which the electric field was turned on and turned off successively with the frequency ω fixed at 10 rad/s. The experiments were repeated at least two or three times for each applied electric field strength to ensure reproducibility.

4.4 Results and Discussion

4.4.1 Characterization of PANI

The FT-IR spectrum of PANI-EB shows five characteristic peaks at 826, 1163, 1307, 1495, and 1584 cm^{-1}. The UV-Vis absorption spectrum of PANI-EB in NMP shows two absorption peaks at 326 and 635 nm. These data confirm that the polyaniline synthesized in our work is similar to previously synthesized emeraldine base (Zeng and Ko, 1998, Huang and MacDiarmid, 1993).

The TGA thermogram of PANI powder measured under N_2 atmosphere shows a 3.15 % weight loss at a temperature between 49.6 and 100 °C, indicative of the evaporation of residual solvent (Li and Wan, 1999).

The PANI particle size and its distribution were determined by a particle size analyzer and we determined that the mean diameter is 23.5 μm with a standard deviation of 2.37 μm. As shown in Figure 4.1, SEM micrograph shows that the shape of the PANI particles and their surfaces are quite irregular. The electrical conductivity of the emeraldine base we prepared is 2.93 x 10^{-9} S/cm, a little smaller than a reported average value in a IUPAC technical report (Stejskal and Gilbert, 2002). As noted in that report, however, reported conductivities of emeraldine base specimens can be as low as 10^{-11} S/cm, in specimens subjected to extensive deprotonation.

4.4.2 Electrorheological Properties of PANI/Silicone Systems

The effects of particle concentration, silicone oil viscosity on ER properties were investigated for four PANI suspensions prepared at volume fractions of 0.024 and 0.048 in silicone oils, with viscosities as listed in Table 4.1. The particle concentrations were chosen to be relatively low to avoid problems due to aggregation of PANI particles in zero electrical field (Gow and Zukoski, 1990), and to facilitate observation of the field driven sol to gel transition (Chin and Winter, 2002). The dedoped (emeraldine base) specimen of PANI (PANI-EB) used in our work was determined to have a conductivity value of 2.93 x 10^{-9} S/cm. PANI of low conductivity was chosen in order to be able to investigate ER behavior at high electric field strength without current leakage in the system. The dynamic moduli, G' and G", were measured in the linear viscoelastic regime as a function of time and frequency. The linear viscoelastic regime was first established via a strain sweep experiment in oscillatory shear at a fixed frequency of 1 rad/s and the electric field strength was varied as shown in Figures 4.2. In the absence of the electric field, G" is significant higher than G' and remains constant to a strain amplitude γ = 500% for all systems except PANI048/100, for which the linear viscoelastic regime shrinks to γ = 20%. As electric field strength is continuously increased, G' becomes larger than G", and the limiting strain amplitude for linear viscoelasticity decreases to very small values γ = 0.3-0.5% at E = 2000 V/mm. As confirmed by optical microscopy, the degree of particle aggregation increases with increasing electric field strength, leading progressively to the formation of particle aggregates, particle strings, and then columns. Accompanying these structural changes, the ER suspension becomes stiffer showing a larger modulus, but also becomes more fragile and is easily fractured at relatively small strains (Chin and Winter, 2002). At higher field strengths, in association with the precipitous decrease in G' above a critical strain, G" increases slightly to a maximum value at a strain level close to that where the viscoelastic response becomes primarily dissipative (tan $\delta \sim 1$). This behavior is very similar to a characteristic nonlinearity observed in the behavior of close-packed colloidal dispersions, when the applied strain becomes sufficient to cause particles to exchange positions with their neighbors, and hence the material can more effectively dissipate the stress (Ketz *et al.*, 1988).

4.4.2.1 Effect of Electric Field Strength and particle concentration

Figures 4.3a and 4.3b show the change in G'(ω) and G"(ω) of PANI024/100 and PANI048/100 suspensions as the electric field is increased in the range 0-2 kV/mm. In the absence of the field, the dynamic moduli exhibit liquid-like behavior such that G" is significantly larger than G' over the entire frequency range. In principle, the frequency dependence should follow $G'(\omega) \propto \omega^2$ and $G''(\omega) \propto \omega$ (Li and Aoki, 1997). Deviations observed from these scaling relations may arise from polydispersity or from flocculational structures formed via interaction between PANI particles (Marshall *et al.*, 1989). When the electric field is applied, the moduli increase by about 5 orders of magnitude, as the electric field strength is increased up to 2 kV/mm. If we define the magnitude of the ER response as ΔG', equal to the value of G'(ω=1) in the absence of the electric field, subtracted from G'(ω=1) with the applied electric field, then, for PANI024/100, ΔG' increases from 0 to 1348 Pa as the field increases from 0 to 2000 V/mm. Comparing PANI024/100 and PANI048/100 at E = 2000 V/mm, an increase of particle concentration by a factor of two results in an equivalent increase in ΔG' from 1348 to 2728 (102 % increase), which is consistent with theoretical expectation (Klingenberg *et al.*, 1991). The suspensions each show solid-like behavior: G' is substantially larger than G" and, at low frequencies, G' becomes independent of frequency (Li and Aoki, 1997).

In the absence of an electric field, the particles are randomly dispersed in suspension. At high fields, the particles form well-developed strings spanning the gap between the electrodes, as a result of interfacial polarization due to migration of charge carriers in the PANI particles (Trilica *et al.*, 2000, Block *et al.*, 1990). Increase in electric field strength induces a higher dipole moment, which causes the particle chains to coalesce and form thicker chains (Chotpattananont *et al.*, 2003). Likewise, higher particle concentration results in a denser fibrillar structure (Cho *et al.*, 2004). The denser, thicker fibrils lead to higher rigidity, manifested in an increase of G'.

4.4.2.2 Effect of host fluid viscosity

The effect of silicone oil viscosity on the ER response of the suspensions was next studied, by comparing results for two oils, having viscosities of

100 and 500 cSt. We present the data in Figure 4a as a plot of values of storage and loss moduli measured at a single frequency of 1 rad/s, designated G'(ω = 1) and G'(ω = 1), versus electric field strength. The results show that the strongest dependence of the shear moduli on the oil viscosity occurs at weak electric field (0 – 400 V/mm) and the dependence becomes less distinct, particularly in the case of the storage modulus, at very high electric field strength (1000 - 2000 V/mm). Thus, at E = 2000 V/mm, ΔG' is 2728 for PANI048/100 and 4103 (50.4% increasing) for PANI048/500. This behavior is very similar to that reported in a recent study of semiconducting ER particles by Sakurai *et al.*, 1990. As noted by these authors, this effect can be explained on the basis that there are two opposing forces contributing to the rheological behavior of the suspension: the electrostatic interparticle force and the hydrodynamic force associated with fluid motion. According to Maxwell-Wagner type-polarization, the electric field will induce in an isolated spherical particle of radius *a*, an electric dipole of magnitude *p*:

$$p = \frac{\pi}{2}\varepsilon_s a^3 \left(\frac{\sigma_p - \sigma_s}{\sigma_p + 2\sigma_s} \right) E_0 = \frac{\pi}{2}\varepsilon_s a^3 \beta E_0 \qquad [1]$$

where E_0 is the electric field strength, and σ_p, σ_s are the electrical conductivities of the particle and matrix, respectively (Davis, 1992), and ε_s is the dielectric constant of the medium. The magnitude of the force between two particles aligned with the electric field and with a center-center separation of *r* is

$$F_{elec} = \frac{3\pi \cdot p^2}{8\varepsilon_s r^4} \qquad [2]$$

On the other hand, in oscillatory shear, at frequency ω and maximum strain γ_o, the maximum value of hydrodynamic force acting to pull each particle apart is (Sakurai *et al.*, 1999)

$$F_{shear} = 6\pi\omega\gamma_0\eta a^2 . \qquad [3]$$

Under weak electric fields, the hydrodynamic force is dominant and the moduli of the suspensions increase as the host fluid viscosity increases. In case of strong fields, a dominant contribution from the interparticle electrostatic force is expected.

Sakurai *et al.* (1999) further note that these observations are consistent with molecular dynamics simulation of an ER fluid under oscillatory shear (Klingenberg, 1993), which indicates the shear moduli (scaled by the electrostatic interaction strength) are functions only of the dimensionless frequency, $\omega^* = (16\eta\omega)/(\varepsilon_s \beta^2 E_0^2)$. Thus the storage modulus should also increase with increasing oil viscosity since the hydrodynamic forces are larger and the chains undergo larger deformations, although this effect should only be seen if the frequency of deformation approaches values high enough to probe a relaxation process associated with the motion of particles in the fibrillar clusters.

4.4.2.3 Sol-gel transition

From the observations in Figures 4.3 and 4.4, it is clear that the ER fluid passes through a liquid-to-solid transition as the electric field increases. Previously, Choi and Winter (2002) identified a sol-gel transition, in an ER suspension composed of monodisperse silica particles, occurring at a critical field strength, by applying the criteria of Chambon and Winter (1986). This involves observation of identical power-law frequency dependence of G' and G", which derives from a power-law relaxation spectrum, originating in a self-similar structure at the gel point. However, we found that this condition did not apply to our data at any point during the field induced increase of G' and G", perhaps due to the wide size polydispersity of our material. As demonstrated by Chin and Winter (2002), the sol-gel transition occurs in ER fluids before the visible formation of particle strings. Chin and Winter (2002) also found, however, that the visible formation of strings correlates to other viscoelastic features emblematic of a liquid-to-solid transition, viz. the appearance of a yield stress and the crossover point of G' and G". Thus, we adopted the criteria G'=G'' to identify the liquid-to-solid transition in our system. As evident in figures 4a and 4b, there is critical electric field strength where G'(1) becomes larger than G" (1). From Figure 4b, we see that, for PANI024/100, the

transition occurs at a higher field strength, E_c = 50 V/mm, compared to PANI048/100 (E_c = 10 V/mm), i.e. the field-driven sol to gel transition occurs more readily at higher concentration.

Likewise, from Fig. 4.4a, comparing suspensions PANI048/500 and PANI048/100, the crossover in G'(1) and G"(1) occurs at a substantially higher critical field strength (E_c = 50 V/mm versus 10 V/mm), for the former sample, which has a higher medium viscosity. Again, this observation can be interpreted in the context of arguments made by Sakurai *et al* (1999), based on the notion that the stronger hydrodynamic forces in the higher viscosity oil enhance the rupturing of stress bearing structures (Davis, 1992). Arguing that the location of the sol-gel transition should scale as the balance between the shear force, F_{shear}, and the electrostatic force, F_{elec}, and utilizing equations (1) – (3), Sakurai et al. deduce the critical field occurs at:

$$E_{crit} = \frac{32}{\pi}\sqrt{\frac{\omega\gamma_o\eta}{\varepsilon_s\beta^2}} \qquad (4)$$

We find that the observed increase in E_c is almost twice as large as predicted by this equation. The origin of the discrepancy is not clear, but may reflect the fact that the critical strain for onset of non-linear behavior decreases as one passes from the sol to the gel state. Also, multi-particle interactions may need to be accounted for to correctly predict the field dependence of the sol-gel transition.

4.4.2.4 Temporal response

Finally, we discuss the temporal response of the PANI suspensions to switching on and off the applied field. Figure 4.5a and 4.5b shows the rheological behavior of the oscillatory complex viscosity, $\eta^* = (1/\omega)\sqrt{(G'^2 + G''^2)}$, together with the maximum strain, of PANI024/100 and PANI048/100 in silicone oil as each suspension is subjected to successive switching of the electric field at increasing field strengths, during a time sweep test with the applied stress fixed at 40 Pa and with the deformation frequency fixed at ω = 1 rad/s. As evident in Figure 5a, the temporal response is very fast to both switching on and off at lower fields. However, at the highest field (3000 V/mm), it is seen that G' does not immediately return to the baseline value, when the field is switched off, and only does so after

some 400 seconds. This indicates that some residual structure persists for some 400 sec after the field is switched off, and implies that the yield stress of this structure is above 40 Pa. As this stress level is maintained on the sample, the structure eventually fatigues and ruptures, in what appears to be two stages of collapse, as evidenced by the stepwise decrease in $\eta*$, and stepwise increase in maximum strain (Figure 4.5b). The static yield stress of the fibrillar structures formed in the presence of the applied field was determined from the onset of steady flow during a controlled stress sweep experiment, as shown in Figure 4.6a, for sample PANI048/100 at three levels of applied field strength. The results are compared with those of the residual structures remaining immediately after the field is turned off (Figure 4.6b), and after 10 minutes of equilibration under field-free and stress-free conditions (Figure 4.6c). The yield stress of the residual structure is an order of magnitude smaller than that of the fully-developed structure in the presence of the field. In Fig.4.7a, the yield stress, τ_y, is plotted against electric field strength for both the equilibrium and residual structures. For the former, we find that $\tau_y \sim E^{1.88}$, very close to the quadratic dependence on field strength as predicted by theoretical models (Parthasarathy and Klingenberg, 1996). For the residual structure, τ_y also increases significantly with field strength but more weakly than for the equilibrium structure, $\tau_y \sim E^{0.98}$. Also shown are τ_y values for the residual structure taken 10 min after the field has been turned off and the sample maintained in a stress-free condition. These delayed τ_y values are significantly smaller than the initial values, particularly at lower field strengths. Evidently, the residual structure decays very slowly, particularly at higher fields.

In Figure 4.7b, we show the dependence of the yield stress on medium viscosity, representing data taken on PANI in three different silicone oils, with viscosities of 100, 500, and 1000 cSt. The results indicate no discernable influence of medium viscosity on τ_y, as indeed expected on the basis that the hydrodynamic force is absent until the onset of flow. At this point, it is pertinent to note that a review of the literature suggests our yield stress values appear to be reasonably consistent with the literature values. For example Gow and Zukoski (1990) reported the yield stress of a 3.75 vol% PANI with a conductivity of 1.47 x

10^{-9} S/cm has a yield stress of about 10 Pa at a field of 1 kV/mm, compared to our value of 20 Pa for a 4.8 wt% PANI with a conductivity of 2.93 x 10^{-9} S/cm.

Finally, Figures 4.8 show the optical micrographs of PANI suspensions at a particle concentration of 0.024% vol at various electric field strengths. It is evident that there is a certain degree of particle aggregation at zero electric field. The aggregates become fibrillar, increase in size and orient along the field direction, as the field strength increases. It is also observed that, in the absence of shear, the field generated structures show no disintegration after the electric field is removed. This result seems consistent with the observation of Gow and Zukoski (1990) that polyaniline suspensions are marginally stable to flocculation, and indeed have a finite yield stress in the absence of an electric field at concentrations higher than those studied in this work.

4.5. Conclusions

PANI emeraldine base particles were synthesized via an oxidative polymerization, followed by dedoping in 3% NH_4OH. The ER properties of PANI/silicone oil suspensions were investigated with respect to the effect of electric field strength, particle concentration, and silicone oil viscosity on dynamic shear moduli, G' and G" and yield stress, τ_y. Consistent with previous observations, the magnitude of the ER response is enhanced with increasing electric field strength and particle concentration. The dynamic moduli, G' and G" increase dramatically, by 5 orders of magnitude, as the electric field strength is increased to 2 kV/mm. A viscoelastic liquid to solid transition occurs at a critical electric field strength, in the range E_c = 50-200 V/mm, whose value increases with particle concentration and decreases with host fluid viscosity. The fibrillar structure formed in the presence of the applied field has a static yield strength τ_y, whose value scales with electric field strength as $\tau_y \sim E^{1.88}$. When the field is switched off a residual structure remains, whose yield stress increases with the strength of the applied field and particle concentration. When the applied stress exceeds the yield stress of the residual structure, fast, fully reversible switching of the ER response is obtained.

4.6 Acknowledgement

The authors would like to acknowledge the financial support provided by The Thailand Research Fund (TRF) in the RGJ grant no. PHD/0234/2544, Conductive & Electroactive Polymers Research Unit, and The Petroleum and Petrochemical Technology Consortium.

4.7 References

Akhavan, J. and Slack, K. (2001). Coating of a semi-conducting polymer for use in electrorheological fluids. Synt. Met., 124, 363-371.

Block, H., Kelly, J.P., Qin, A., and Watson, T. (1990). Materials and mechnisma in electrorheology. Langmuir, 6, 6-14.

Cao,Y., Andreatta, A., Heeger, A.J., and Smith,P. (1989). Influence of chemical polymerization conditions on the properties of polyaniline. Polymer, 30, 2305-2311.

Chin, B.D. and Winter, H.H. (2002). Field-induced gelation, yield stress, and fragility of an electro-rheological suspension. Rheol. Acta., 41, 265-275.

Chin, B.D., Lee, Y.S., and Park, O.O. (1998). Effect of conductivity and dielectric behavior on the electrorheological response of a semiconductive poly(p-phenylene) suspension. J. Colloid Interface Sci., 201, 172-179.

Cho, M.S., Lee, J.H., Choi, H.J., Ahn, K.H., and Lee, S.J. (2004). Linear viscoelasticity of semiconducting polyaniline based electrorheological suspensions. J. Mater. Sci., 39, 1377-1382.

Choi, H.J., Cho, M.S., and To, K. (1998). Electrorheological and dielectric characteristics of semiconductive polyaniline-silicone oil suspensions. Physica A., 254, 272-279.

Chotpattananont, D., Sirivat, A., and Jamieson, A. M. (2004). Scaling of yield stress of polythiophene suspensions under electric field. Macromol. Mat. Eng., 289, 434-441.

Chotpattananont, D., Sirivat, A., and Jamieson, A.M. (2003). Electrorheological properties of perchloric acid-doped polythiophene suspensions. Colloid Polym. Sci., 282, 357-365.

Davis, L.C. (1992). Polarization forces and conductivity effects in electrorheological fluids. J. App. Phys., 72, 1334-1340.

Gow, C. J. and Zukoski, C. F. (1990). The electrorheological properties of polyaniline suspensions. J. Coll. Interf. Sci., 136, 175-188.

Gozdalik, A., Wycislik, H., and Plocharski, J. (2000). Electrorheological effect in suspensions of polyaniline. Synt. Met., 109, 147-150.

Huang, W.S. and MacDiarmid, A.G. (1993). Optical properties of polyaniline. Polymer, 34, 1833-1845.

Jang, W.H., Kim, J.W., Choi, H.J., and Jhon, M.S. (2001). Synthesis and electrotheology of camphorsulfonic acid doped polyaniline suspensions. Colloid. Polym. Sci., 279, 823-827.

Ketz, R., Prudhomme, R. K. and Graessley, W. W. (1988). Rheology of concentrated microgel solutions. Rheol. Acta, 27, 531-539.

Kim, S.G., Kim, J.W., Choi, H.J., Suh, M.S., Shin, M.J., and Jhon, M.S. (2000). Synthesis and electrorheological characterization of emulsion-polymerized dodecylbenzenesulfonic acid doped polyaniline-based suspensions. Coll. Polym. Sci., 278, 894-898.

Klingenberg, D. J. Swol, F. V. and Zukoski,C. F. (1991). The small shear rate response of electrorheological suspensions. 1 Simulation in the point-dipole limit. J. Chem. Phys., 94, 6160-6169.

Klingenberg, D.J. (1993). Simulation of the dynamic oscillatory response of electrorheological suspensions: demonstration of relaxation mechanism. J. Rheol., 37, 199-214.

Klingenberg, D.J., Zukoski, C.F., and Hill, J.C. (1993). Kinetics of structure formation in electrorheological suspensions. J. Appl. Phys., 73, 4644-4648.

Lee, H.-J., Byung, D.C., Yang, S.-M., and Park, O.O. (1998). Surfactant effect on the stability and electrorheological properties of polyaniline particle suspension. J.Colloid. Interface. Sci., 206, 424-438.

Lee, Y.H., Kim, C.A., Jang, W.H., Choi, H.J., and Jhon, M. (2001). Synthesis and electrorheological characteristics of microencapsulated polyaniline particles with melamine-formaldehyde resins. Polymer., 42, 8277-8283.

Lengalova, A., Pavlinek, V., Saha, P., Quadrat, O.,Stejskal, J. (2003). The effect of dispersed particle size and shape on the electrorheological behavior of suspensions. Euro. Polym. J., 39, 641-648.

Li, L. and Aoki, Y. (1997). Rheological images of poly(vinyl chloride) gels. 1. The dependence of sol-gel transition on concentration. Macromolecules, 30, 7835-7841.

Li, W. and Wan, M. J. (1999). Stability of polyaniline synthesized by a doping-dedoping-redoping method. Appl. Polym. Sci., 71, 615-621.

Marshall, L., Zukoski IV, C.F., and Goodwin, J.W. (1989). Effects of electric field on the rheology of non-aqueous concentrated suspensions. J. Chem. Soc. Faraday Trans.1, 85, 2785-2795.

Parthasarathy, M. and Klingenberg, D. J. (1996). Electrorheology: mechanisms and models. Mater. Sci. Eng., R17, 57-103.

Pinto, N.J., Acosta, A.A., Sinha, G.P., and Aliev, F.M. (2000). Dielectric permittivity study on weakly doped conducting polymers based on polyaniline and its derivatives. Syn. Met., 113,77-81.

rilica,J., Saha, P., Quadrat, O., and Stejskal, J. (2000). Electrorheology of polyaniline-coated silica particles in silicone oil. J. Phys.D: Appl. Phys., 33, 1773-1780.

Sakurai, R., See, H., Saito, T., and Sumita, M.(1999). Effect of matrix viscoelasticity on the electrorheological properties of particle suspensions. J. Non-Newtonian Fluid Mech., 81, 235-250.

Sim, I.S., Kim, J.W., Choi, H.J., Kim, C.A., and Jhon, M.S. (2001). Preparation and electrorheological characteristics of poly(p-phenylene)-based suspensions. Chem. Mater., 13, 1243-1247.

Stejskal, J. and Gilbert, R.G. (2002) Polyaniline. Preparation of a conductive polymer. Pure Appl. Chem., 74, 857-867.

Tao, R. and Sun, J.M. (1991).Three-dimensional structure of induced electrorheological solid. Phys. Rev. Lett., 67, 398-438.

Winter, H. H. and Chambon, F. (1986). Analysis of linear viscoelasticity of a crosslinking polymer at the gel point. J. Rheol., 30, 367-382.

Zeng, X.-R. and Ko, T.-M. (1998). Structures and properties of chemically reduced polyanilines. Polymer, 39, 1187-1195.

Table 4.1 Properties of dedoped PANI suspensions in silicone oil with electrical conductivity value of PANI particle of 2.93 x 10^{-9} S/cm

Code	Particle concentration (vol%)	Silicone oil viscosity (cSt)
PANI024/100	**2.4**	**100**
PANI048/100	**4.8**	**100**
PANI048/500	**4.8**	**500**
PANI048/1000	**4.8**	**1000**

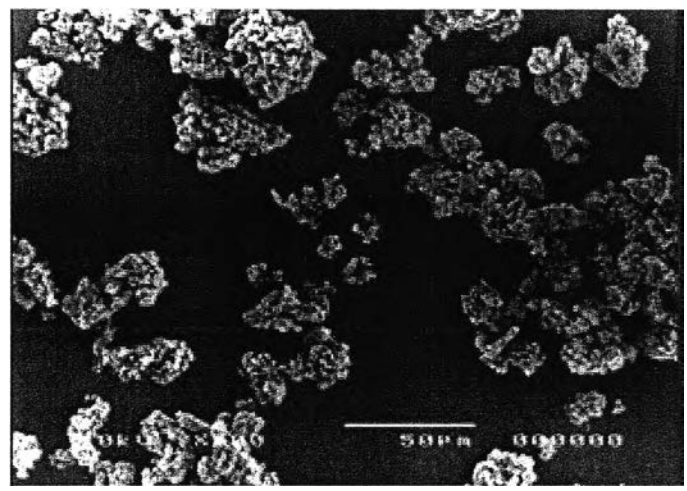

Figure 4.1 Scanning electron microscopy of polyaniline (emeraldine base) particles, average particle size is 23.5 μm.

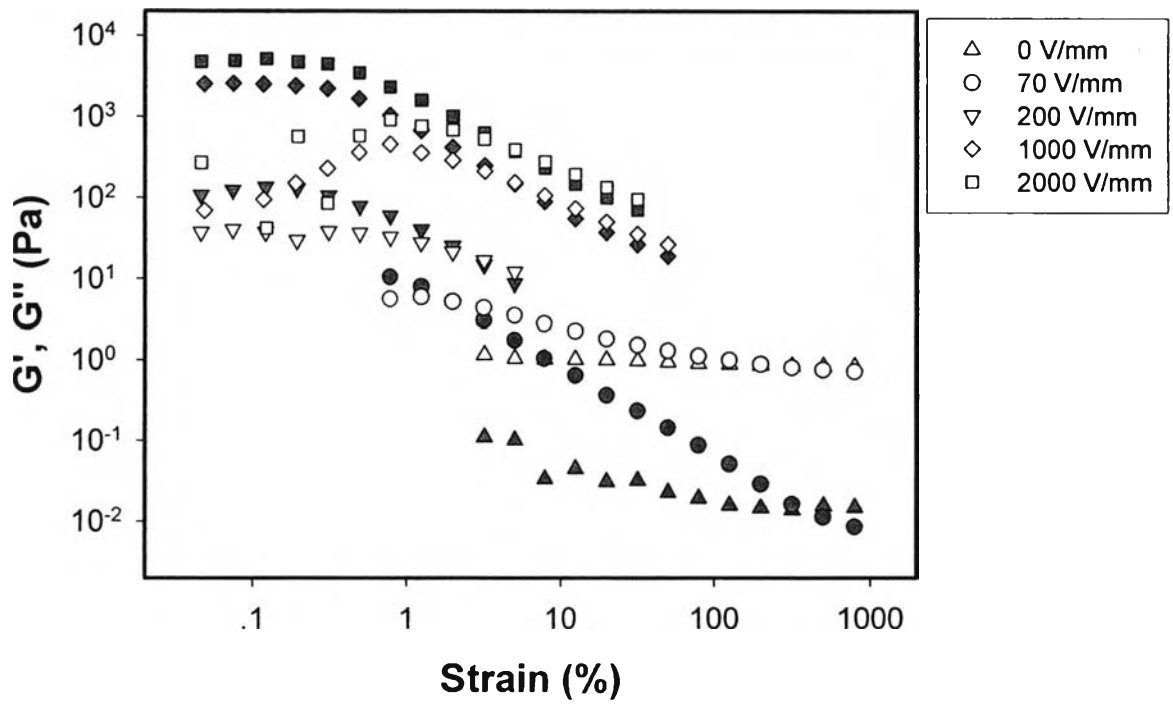

Figure 4.2 Strain dependence of G' and G" for PANI048/500 at temperature of 25 ± 1 °C. Gap = 0.399-0.558 mm, frequency = 1 rad/s: open symbols for G' and shaded symbols for G".

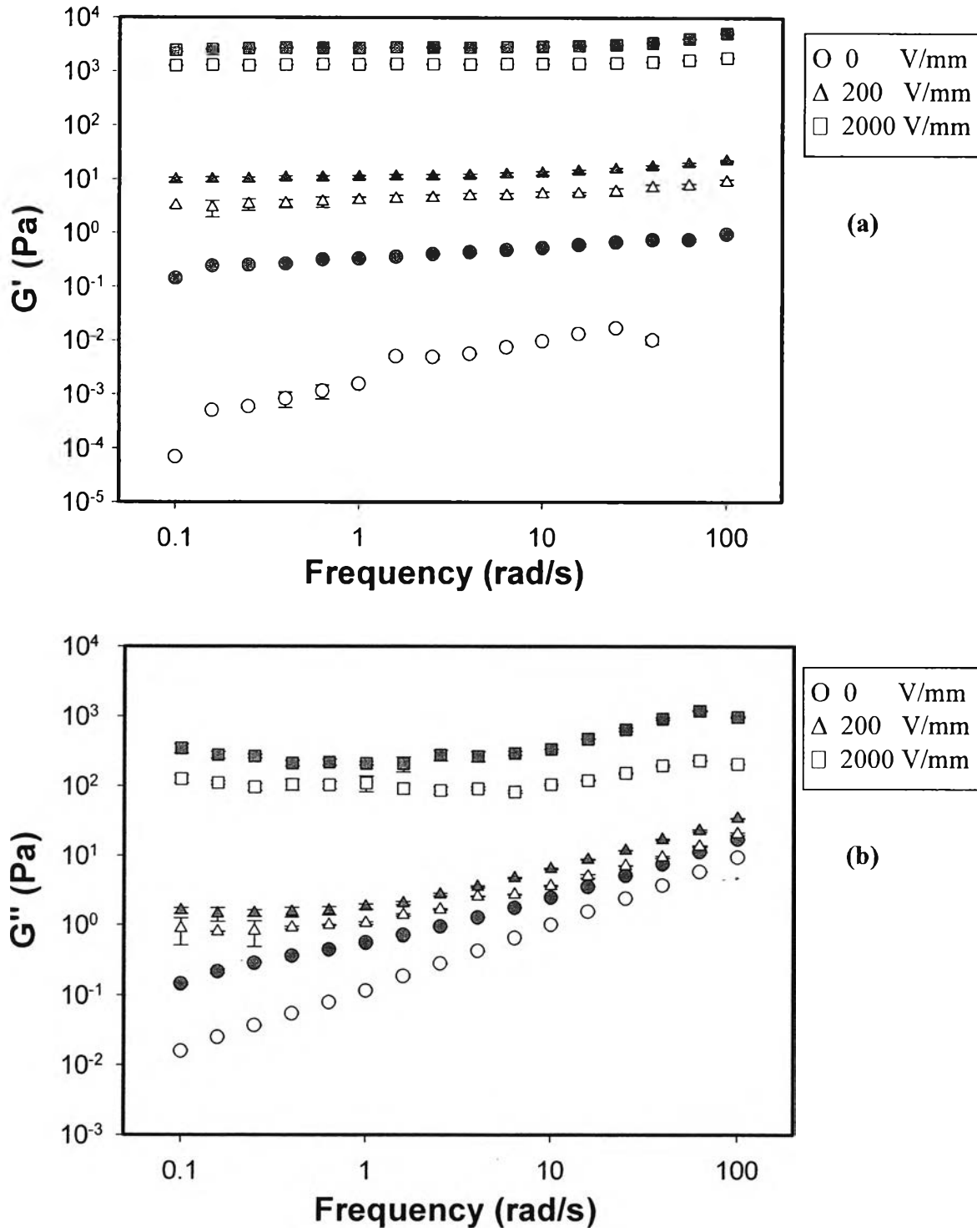

Figure 4.3 Frequency dependence of shear moduli of PANI /Silicone oil suspension: **(a)** storage modulus, G'; **(b)** loss modulus, G", at temperature of 25 ± 1 °C. Gap = 0.399-0.558 mm, strain 0.3-500%: open symbols, ○ △ □ for PANI024; shaded symbols, ● ▲ ■ for PANI048.

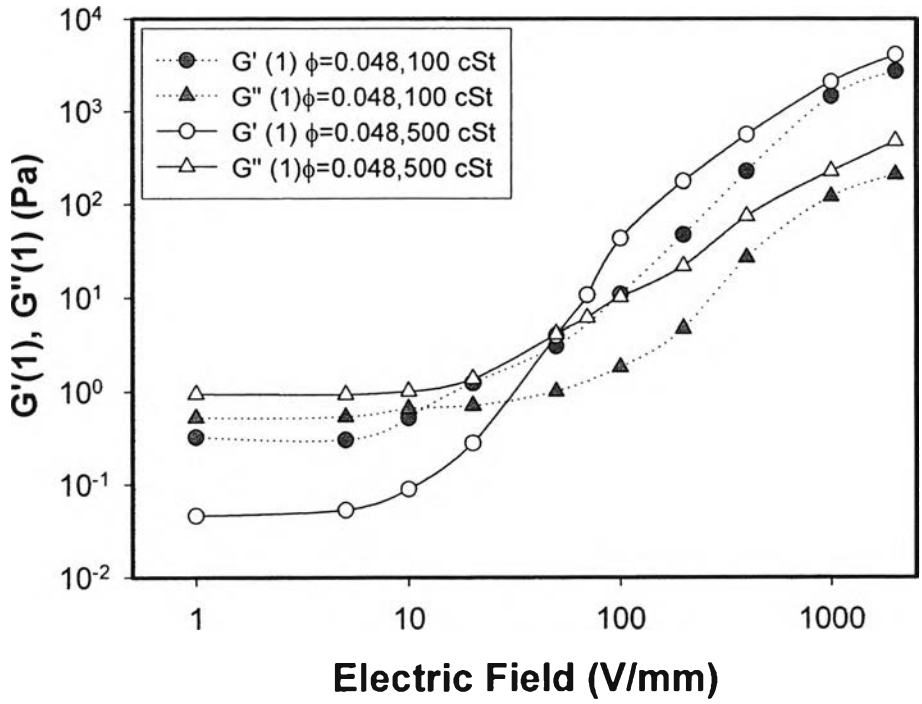

(a)

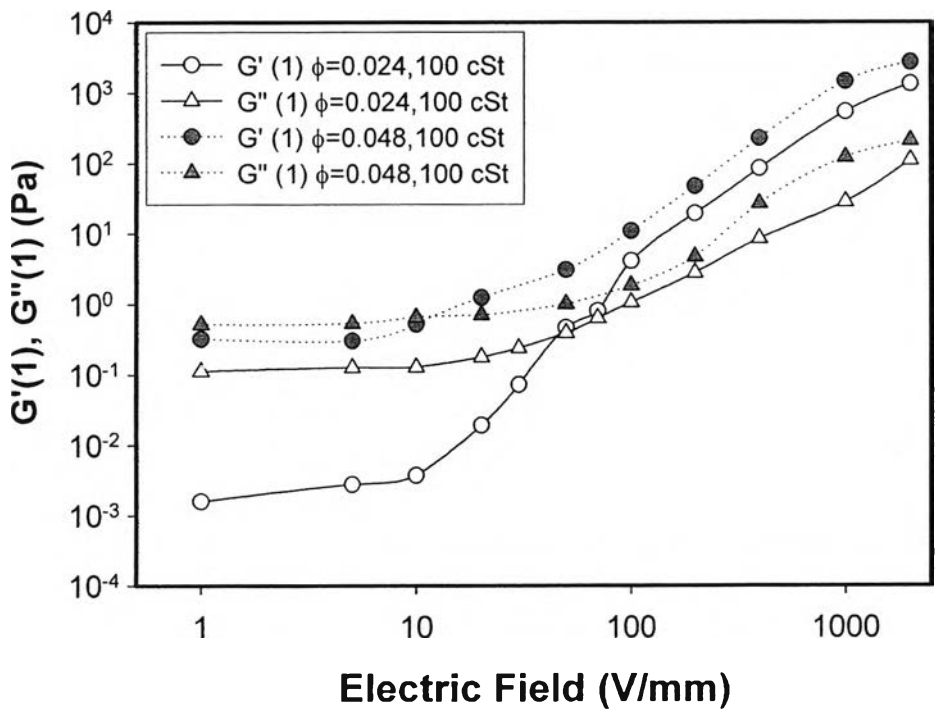

(b)

Figure 4.4 Electric field dependence of G' and G" measured at frequency 0.1 rad/s: **(a)** effect of silicone oil viscosity, open symbols are for η = 100 cSt; shaded symbols are for η = 500 cSt; **(b)** effect of particle concentration, open symbols for PANI024/100; shaded symbols are for PANI048/100.

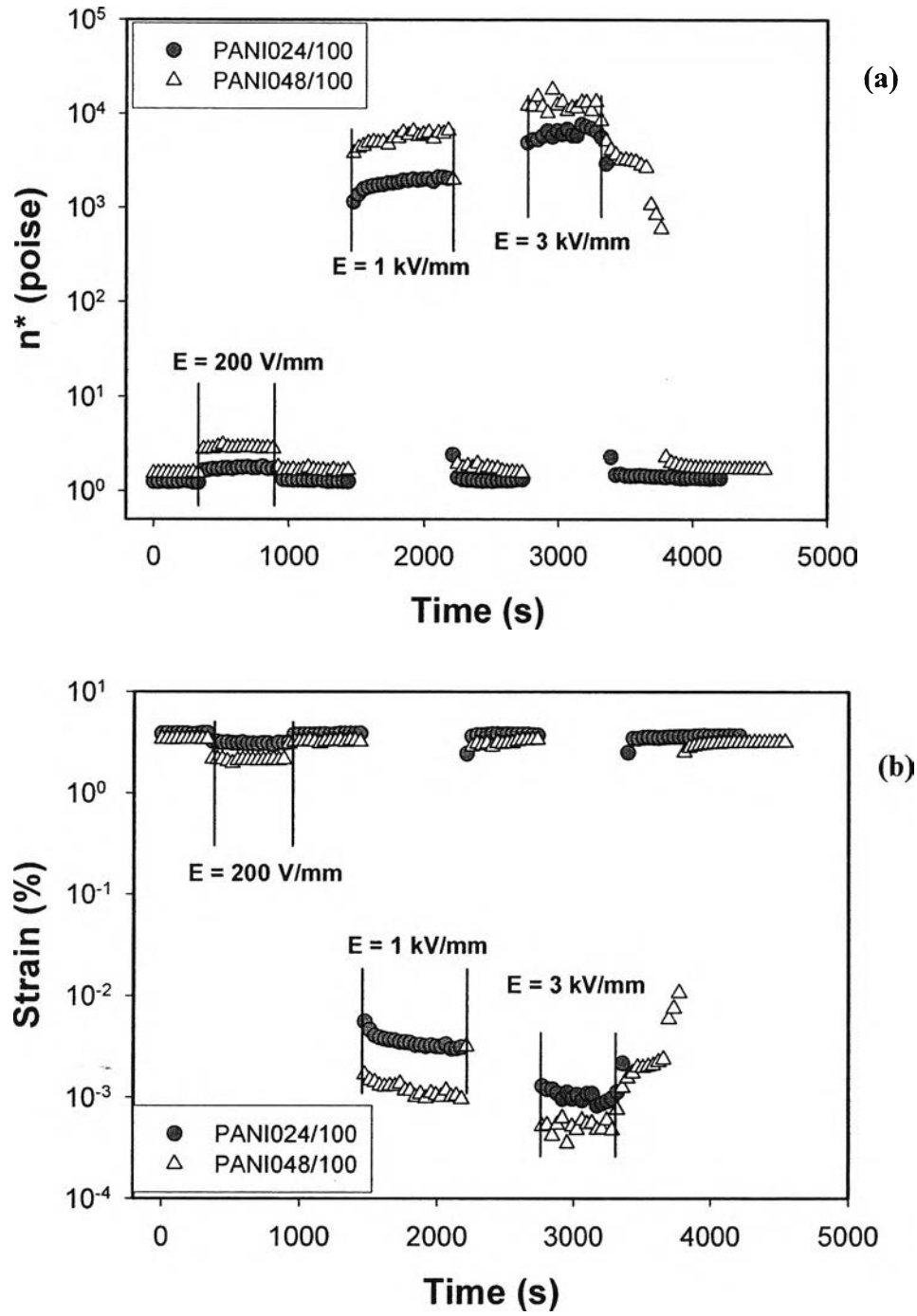

Figure 4.5 Temporal ER switching response of 2.4 % and 4.8 %vol PANI/Silicone oil suspensions (PANI024/100 and PANI048/100) at various electric field strengths. Gap = 0.2 mm, stress 40 Pa, temperature 25 °C: **(a)** complex viscosity, η*; **(b)** the shear strain.

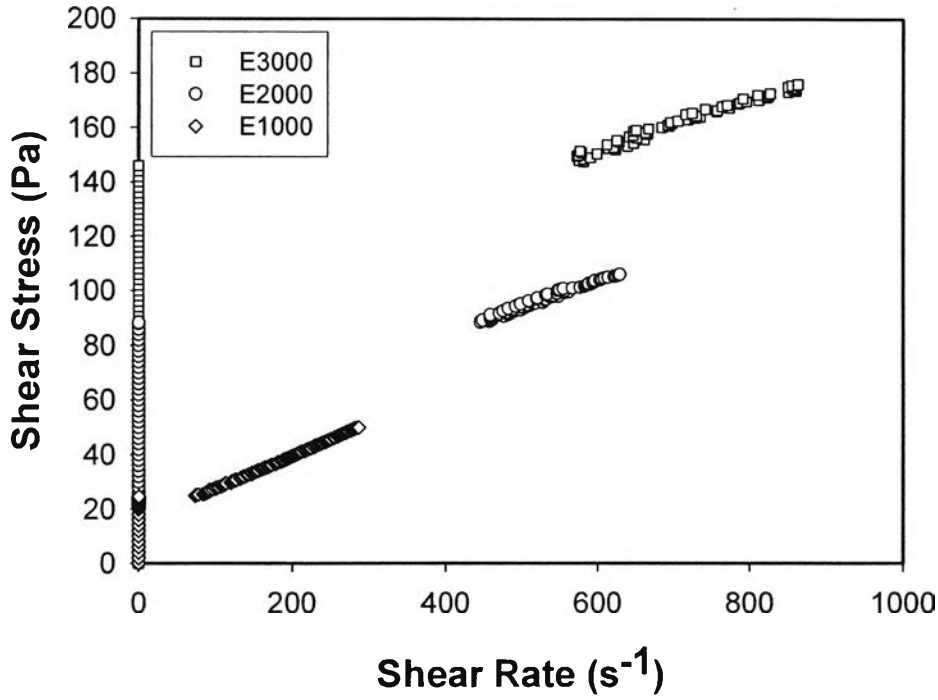
E3000
E2000
E1000
Shear Stress (Pa)
Shear Rate (s-1)
0
20
40
60
80
100
120
140
160
180
200
0
200
400
600
800
1000

(a)

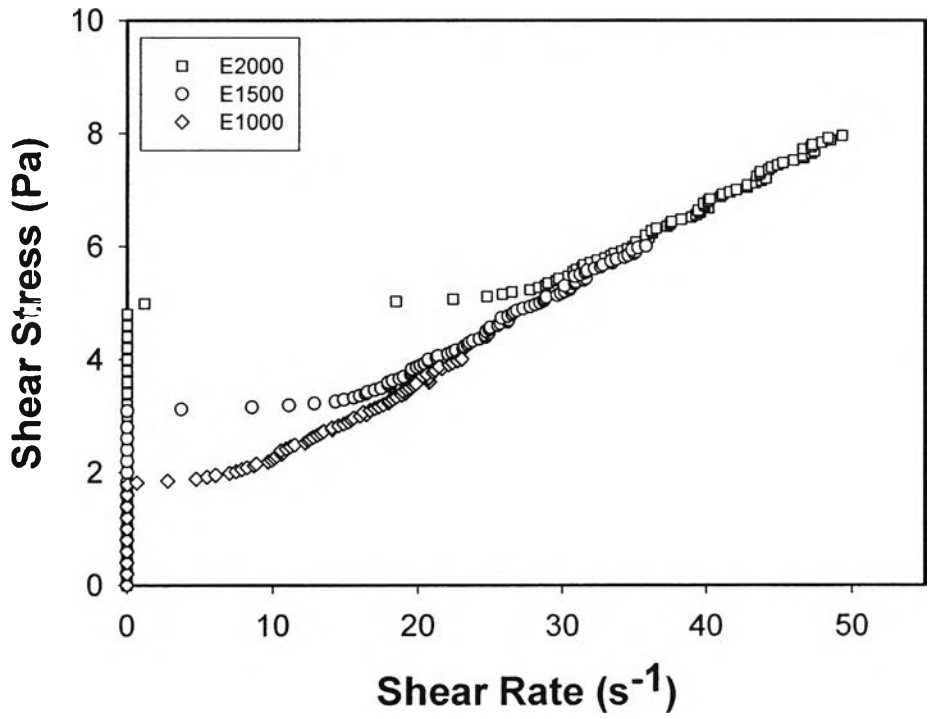
E2000
E1500
E1000
Shear Stress (Pa)
Shear Rate (s-1)
0
2
4
6
8
10
0
10
20
30
40
50

(b)

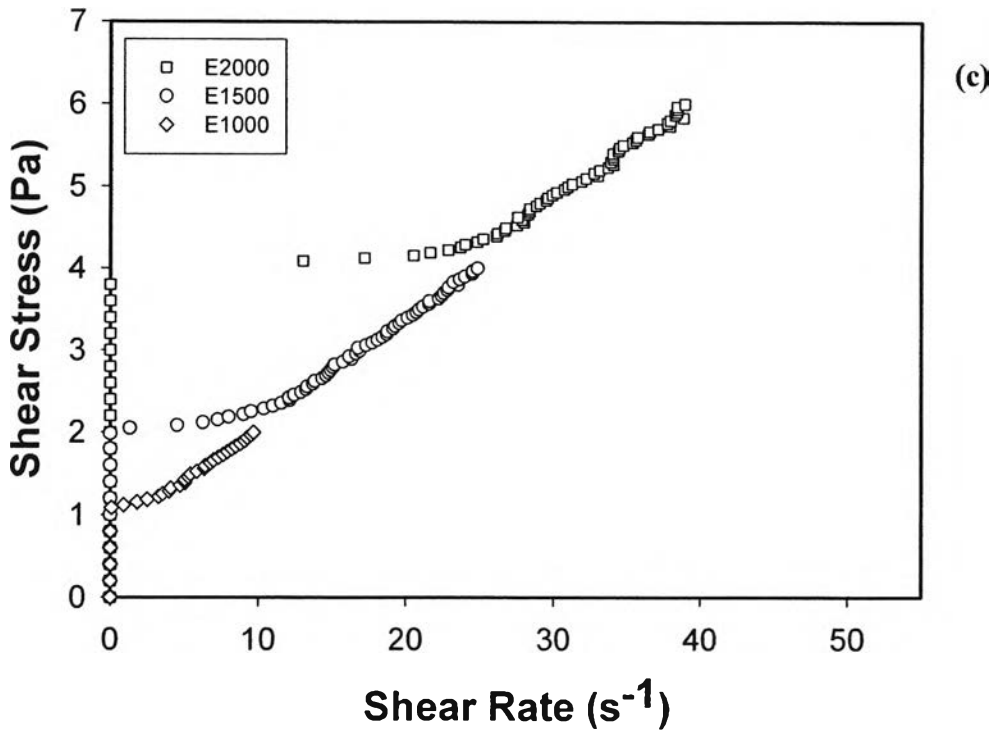

Figure 4.6 Measurement of the static yield stress at different electric field strengths for PANI048/100 at 25°C: **(a)** equilibrium structure under electric field; **(b)** measured immediately after the electric field was switched off; and **(c)** measured 10 minutes after the electric field was switched off.

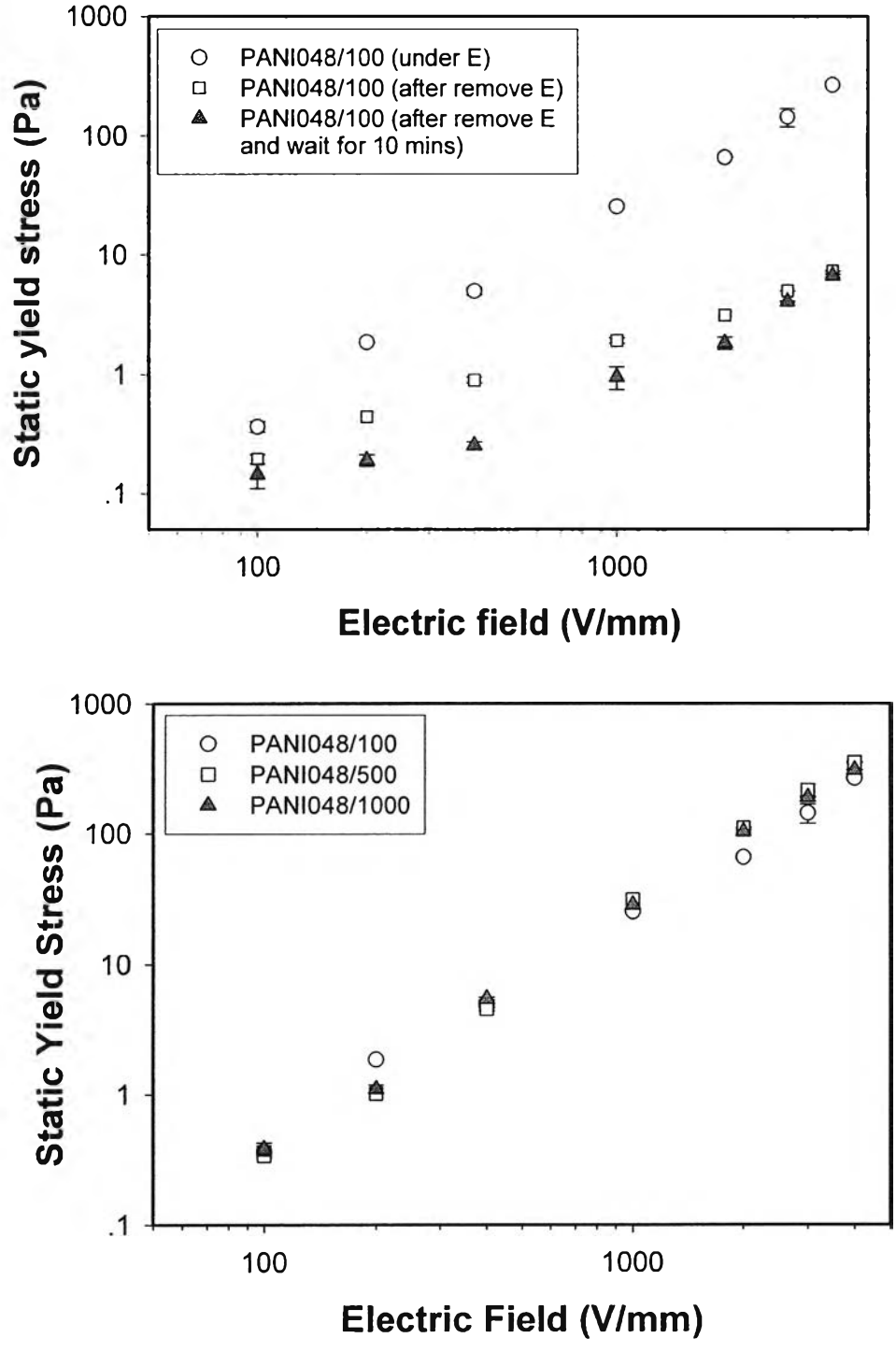

Figure 4.7 Static yield stress of PANI /Silicone oil suspension: **(a)** ● measured in the presence of an electric field, ▲ measured immediately after the electric field was switched off, and ○ measured 10 minutes after the electric field was switched off; **(b)** ○ for PANI048/100, □ for PANI048/500, and ▲ for PANI048/1000.

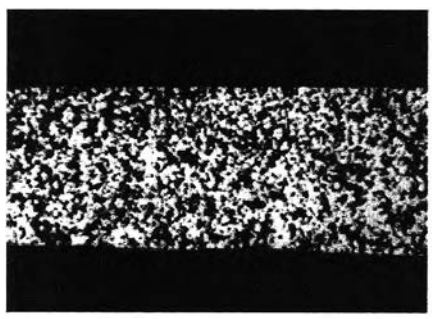

E = 0 kV/mm

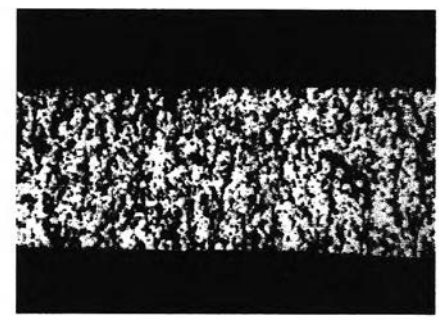

E = 0.2 kV/mm

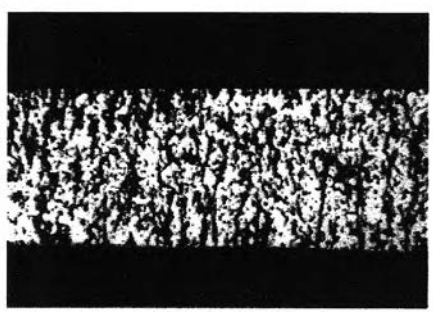

E = 1 kV/mm

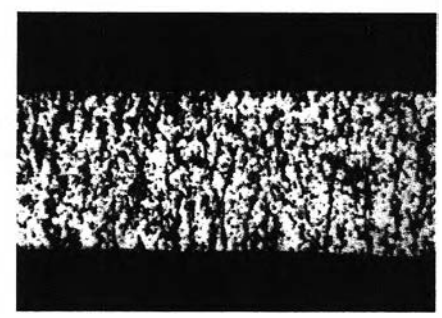

After E = 1 kV/mm was removed for 30 mins

Figure 4.8 Optical micrographs of PANI024/100 at 25°C at various electric field strengths.